

Vertical nanopillars for *in situ* probing of nuclear mechanics in adherent cells

Lindsey Hanson¹, Wenting Zhao², Hsin-Ya Lou¹, Ziliang Carter Lin³, Seok Woo Lee², Praveen

Chowdary¹, Yi Cui^{2,4*}, Bianxiao Cui^{1*}

¹Department of Chemistry, ²Department of Materials Science and Engineering, and ³Department of Applied Physics, Stanford University, Stanford, California 94305

⁴Stanford Institute for Materials and Energy Sciences, SLAC National Accelerator Laboratory, 2575 Sand Hill Road, Menlo Park, California 94025

* To whom correspondence should be addressed. E-mail: BC, bcui@stanford.edu; YC, yicui@stanford.edu

Cell culture and transfection

NIH 3T3 were cultured in 10% FBS and 1% penicillin-streptomycin in DMEM. Chinese hamster ovary (CHO) cells were cultured in 10% FBS and 1% penicillin-streptomycin in F12K medium. HL1 cells were cultured in 10% horse serum and 1% penicillin-streptomycin in Claycomb medium. Primary hippocampal neurons were dissected from E18 rat embryos according to previously published protocols⁵⁸ and cultured in Neurobasal medium supplemented with B27 and 1% penicillin-streptomycin.

For live imaging, cells were transfected with GFP-Sun2, a GFP-tagged inner nuclear membrane protein³⁹, or GFP-lamin A (Addgene plasmid 17662), a GFP-tagged intermediate filament in the nuclear lamina⁵⁹, in order to fluorescently label the nuclear envelope. For nuclear stiffness tests, 3T3 cells were transfected with either GFP-lamin A (Addgene plasmid 17662) or GFP-progerin⁵⁹ (Addgene plasmid 17663). The cells were first starved in serum-free minimal medium (OPTI-MEM) for 30 minutes, while 1 µg of plasmid was mixed with 3 µl lipofectamine in OPTI-MEM and incubated at room temperature for 20 minutes. The medium was then exchanged for the transfection mixture, and the cells were incubated in said mixture for three hours at 37°C. The transfection mixture was replaced by culture medium and the cells are allowed to recover overnight before imaging.

TEM sample preparation

All chemicals for the TEM preparation were purchased from Electron Microscopy Sciences unless otherwise noted. After 2-3 days in culture, the cells were fixed in 2% glutaraldehyde and 4% PFA in 0.1 M sodium cacodylate buffer (pH 7.3) at room temperature for 30 minutes followed by fixation at 4°C overnight. The following steps were carried out at 4°C until warming to room temperature during the graded ethanol series. The sample was washed in 0.1 M sodium cacodylate buffer, and post-fixed in 1% osmium tetroxide in 0.1 M sodium cacodylate buffer. After washing three times with distilled water, the sample was en-bloc stained with 2% uranyl acetate, washed three times again with distilled water, and dehydrated in a graded ethanol series. Subsequently, the 100% ethanol (Gold Shield) was exchanged for acetonitrile. This was followed by infiltration with a 1:1 mixture of acetonitrile and Embed 812 resin for 1.5 hours, and a 1:2 mixture of acetonitrile and resin overnight. The resin-acetonitrile

mixture was then replaced with pure resin, which was allowed to infiltrate the sample for three hours. This was exchanged again for fresh pure resin, incubated at room temperature for 1.5 hours, and baked at 65°C for 24 hours. The quartz coverslip was etched away by 49% hydrofluoric acid (Avantor), and the resin was thoroughly washed and then dried at 65°C. The sample was then re-embedded with fresh pure resin to refill the spaces left by the coverslip and baked for 24 hours. The resin block was then trimmed and sectioned on a Leica Ultracut ultramicrotome into 70nm-thick sections. The sections were collected on 1x2mm copper slot grids with carbon-formvar support film (Electron Microscopy Sciences) and post-stained for 30 seconds in 1:1 uranyl acetate:acetone. The grids were imaged at 120kV on a Jeol 1400 TEM.

Immunostaining and fluorescence imaging

Cells cultured on nanopillar substrates were immunostained for lamin A and actin. Cells were washed with pre-warmed PBS and fixed in 4% PFA in PBS for 10 minutes. The cells were then washed three times with PBS, permeabilized with 1% Triton X-100 in PBS for 5 minutes, and washed again three times with PBS. Samples were blocked with staining buffer (1% BSA and 0.3% Triton X-100 in PBS) for 30 minutes before staining with 1:200 anti-lamin A (Millipore MAB3540) or 1:500 anti-nuclear pore complex (Abcam, Mab414, Cat# ab24609) in the same solution. Samples were washed five times with staining buffer and stained with the secondary antibody, goat anti-mouse IgG Alexa 488 (Life Technologies A11001), 1:500 in staining buffer for 30 minutes. For actin staining, a second staining was performed with 1:500 phalloidin-Alexa568 (Life Technologies A12380).

Samples were imaged on an Olympus FV1000 laser-scanning confocal microscope. A 100 μm aperture was used with a 60X water immersion objective (NA 1.20), and z-slices were acquired every 0.1 μm . Pixel dwell time was 20 μs and all data was acquired in photon count mode. For live imaging, samples were imaged in an on-stage incubator on a Leica DMI6000B inverted microscope using a 100X oil-immersion objective.

Calculation of peak fitting accuracy

The standard error of the peak center was calculated from experimental data according to the method of Thompson et al⁴¹. Specifically, the equation

$$\langle(\Delta x)^2\rangle = \frac{s^2}{N} + \frac{a^2/12}{N} + \frac{4\sqrt{\pi}s^3b^2}{aN^2}$$

represents the mean square error of localization in one dimension, where s is the standard deviation of the peak, a is the pixel size, b is the standard deviation of the background, and N is the number of photons collected per peak. To describe our experimental setup, we used the value 1000 nm for the standard deviation of the peak, 100 nm for the pixel size, 10 photons for the standard deviation of the background (measured from background pixels), and 10^4 for the median number of photons collected per peak. This gave us a root mean square error of 20 nm.

To validate that accuracy experimentally, we tested our Z localization on a supported lipid bilayer on a glass coverslip. Lipid vesicles were prepared from egg PC with 1% Texas Red-DHPE and extruded through 100 nm filters. The glass coverslip was cleaned by air plasma for 1 hour and immediately incubated with the vesicles for 5 minutes before washing with PBS. The sample was kept in PBS and imaged on the confocal fluorescence microscope under the same conditions as a cell sample, except for the use of a 559 nm laser to excite Texas Red. The confocal stack was used to determine the Z position at each pixel (Supplementary Figure 3a). The root mean square deviation of the calculated Z positions was 60 nm (Supplementary Figure 3b). The difference can be mostly accounted for by the lower signal we obtained from the lipid bilayer, as the number of photons collected was about ¼ that from the typical nucleus staining.

Finite element analysis

We performed finite element analysis with COMSOL Multiphysics (COMSOL Inc.) to demonstrate the deformation of the nucleus on the nanopillar. In order to appropriately approximate our system, we created a 4 µm-thick nucleoplasm bordered above and below by a nuclear envelope, which included the combined mechanical properties⁵⁶ of the nuclear lamina and both nuclear membranes. These layers were combined according to the equation:

$$\text{Young's modulus, } E_{memb} = \frac{E_b^2 t_b^4 + E_{NL}^2 t_{NL}^4 + 2E_b E_{NL} t_b t_{NL} (2t_b^2 + 3t_b t_{NL} + 2t_b^2)}{(E_b t_b + E_{NL} t_{NL})(1 - \nu) t_{memb}^3}$$

where E_b and E_{NL} signify the young's modulus of the nuclear envelope and the nuclear lamina, respectively, and t_b and t_{NL} represent their respective thicknesses. E_{memb} and t_{memb} indicate the combined effective Young's modulus and thickness of the merged nuclear envelope. See Supplementary Table S1 for values of mechanical properties used.

This nucleus structure was placed atop a nanopillar with a given radius, and the size of the square nucleus above was determined by the pitch of the desired array. The deformation of the nanopillar for the applied pressure in the simulation is negligible since its Young's modulus is five orders larger than the membrane. The nanopillar was topped with a soft cap, which was 500 nm thick to match the final distance between the nucleus and nanopillar in our TEM studies and had a Young's modulus⁶⁰ of 250 Pa, in order to simulate the cytoplasm. This cap did not have an effect on the overall trends in deformation, as it simply allowed a net displacement downward. Periodic boundary conditions were established requiring the nuclear envelope to be parallel to the substrate at the boundary.

Pressure was then applied to the lower surface of the nucleus, according to the three models detailed in the main text: uniform, localized, and combined (uniform + localized). For the pitch dependence simulations, a nanopillar with a radius of 300 nm was used, and the pitch was varied from 2 μm to 3 μm , 5 μm , and 6 μm . In each case, the pressure was held constant as we varied the nanopillar pitch. The amplitudes of each pressure model were chosen to match the experimental indentation depth on a nanopillar with a radius of 300 nm and pitch of 6 μm , because at that large pitch the nanopillar-induced deformations can be assumed to be independent from each other. The uniform pressure applied was 1.35 Pa. Localized pressures had a Gaussian profile with a standard deviation of 0.51 μm to match the width of the actin accumulation we observed in fluorescence staining, and the maximum pressure was 90 Pa. For the combined pressure model, the uniform pressure (P_U) and the localized pressure (P_L) were scaled and added such that the total pressure remained the same as in each of the other pressure models. That is, the combined pressure (P_C) was determined as $P_C = \alpha P_U + (1-\alpha)P_L$, where α is a

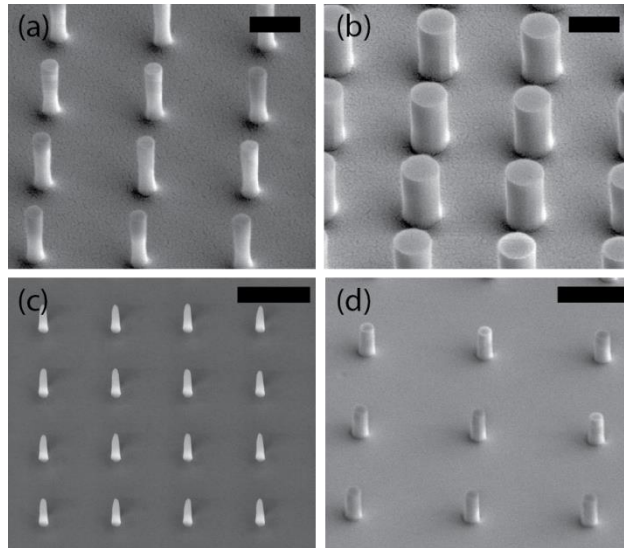
proportionality constant optimized to best match the experimental data but held constant for all nanopillar pitches. The final pressures applied in the combined pressure model with $\alpha = 0.65$ amounted to 0.9 Pa of uniform pressure and a localized Gaussian pressure with a maximum of 35 Pa. In the calculation, linear elasticity of the materials is considered and displacement along z direction is plotted for the applied pressure.

Supplementary Table S1. Sample sizes for each experiment.

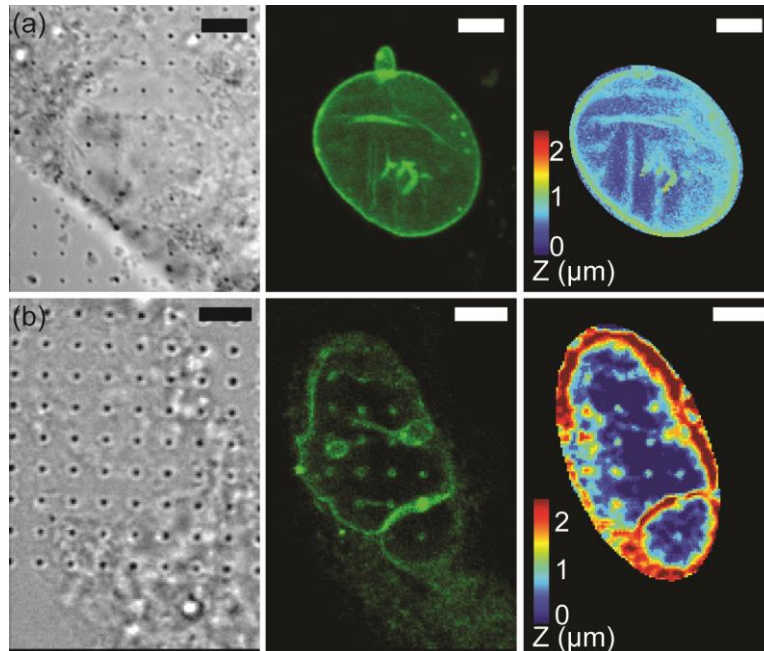
Sample	Number of Nanopillars	Number of Nuclei	Sample	Number of Nanopillars	Number of Nuclei
Figure 3b, Untreated 3T3 r=100 nm	76	29	Figure 3c, Untreated 3T3	547	233
Figure 3b, Untreated 3T3 r=175 nm	173	67	Figure 3c, 3T3+lamin A	125	29
Figure 3b, Untreated 3T3 r=225 nm	182	73	Figure 3c, 3T3+progerin	47	13
Figure 3b, Untreated 3T3 r=300 nm	116	64	Figure 3f, Untreated 3T3	1548	365
Figure 3b, 3T3+lamin A r=100 nm	38	7	Figure 3f, HL1	115	40
Figure 3b, 3T3+lamin A r=175 nm	28	9	Figure 3f, MCF7	851	43
Figure 3b, 3T3+lamin A r=225 nm	34	6	Figure 3f, Neurons	176	37
Figure 3b, 3T3+lamin A r=300 nm	25	7			

Sample	Number of Nanopillars	Number of Nuclei	Sample	Number of Nanopillars	Number of Nuclei
Figure 4b, Untreated 3T3	182	73	Figure 5b, r=230nm	155	25
Figure 4b, 3T3+LatB	65	17	Figure 5b, r=300nm	129	27
Figure 4b, 3T3+Colchicine	143	32	Figure 5b, r=350nm	167	25
Figure 4b, 3T3+Acrylamide	261	41	Figure 5c, r=100nm	76	29
Figure 4c, Untreated 3T3	116	64	Figure 5c, r=175nm	173	67
Figure 4c, 3T3+LatB	63	21	Figure 5c, r=225nm	182	73
Figure 4c, 3T3+Colchicine	80	19	Figure 5c, r=300nm	116	64
Figure 4c, 3T3+Acrylamide	263	47	Figure 5e-f, pitch=2μm	129	27
Supp Fig S6, 3T3+CytoD	118	28	Figure 5e-f, pitch=3μm	116	64
Figure 5b, r=75nm	225	33	Figure 5e-f, pitch=5μm	26	17
Figure 5b, r=150nm	360	41	Figure 5e-f, pitch=6μm	44	37

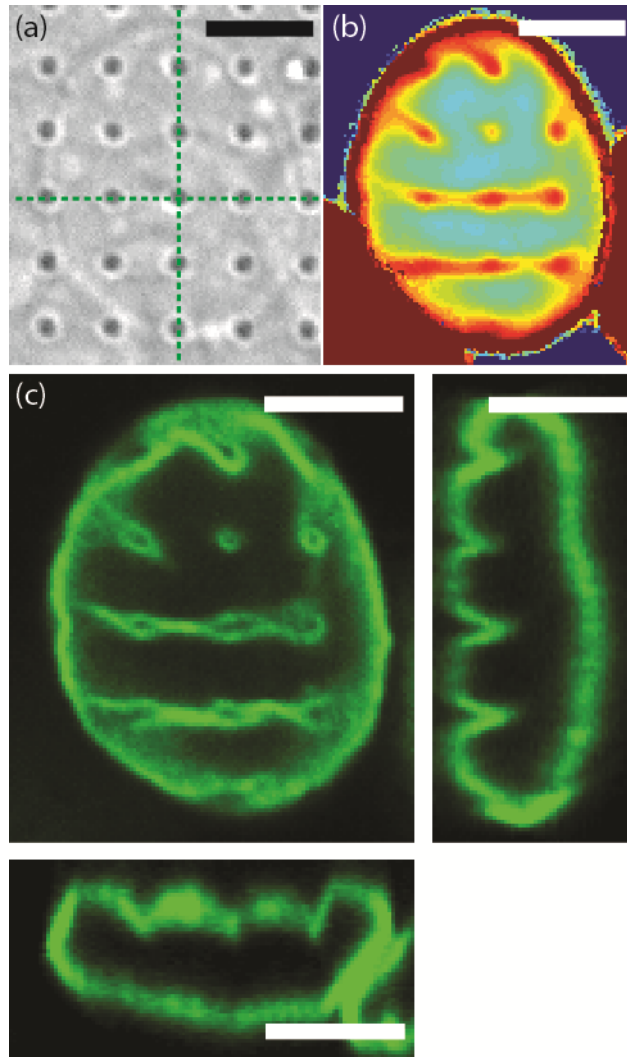
Supplementary Figure S1 Nanopillar dimensions are examined by scanning electron microscopy after fabrication. Pitch, radius and height are varied between different samples. (a) 2 μm pitch, 75 nm radius, 1.4 μm height. Tilt 45°. Scale bar 1 μm . (b) 2 μm pitch, 350 nm radius, 1.4 μm height. Tilt 45°. Scale bar 1 μm . (c) 3 μm pitch, 150 nm radius, 2 μm height. Tilt 30°. Scale bar 3 μm . (d) 6 μm pitch, 300 nm radius, 1.4 μm height. Tilt 45°. Scale bar 3 μm .



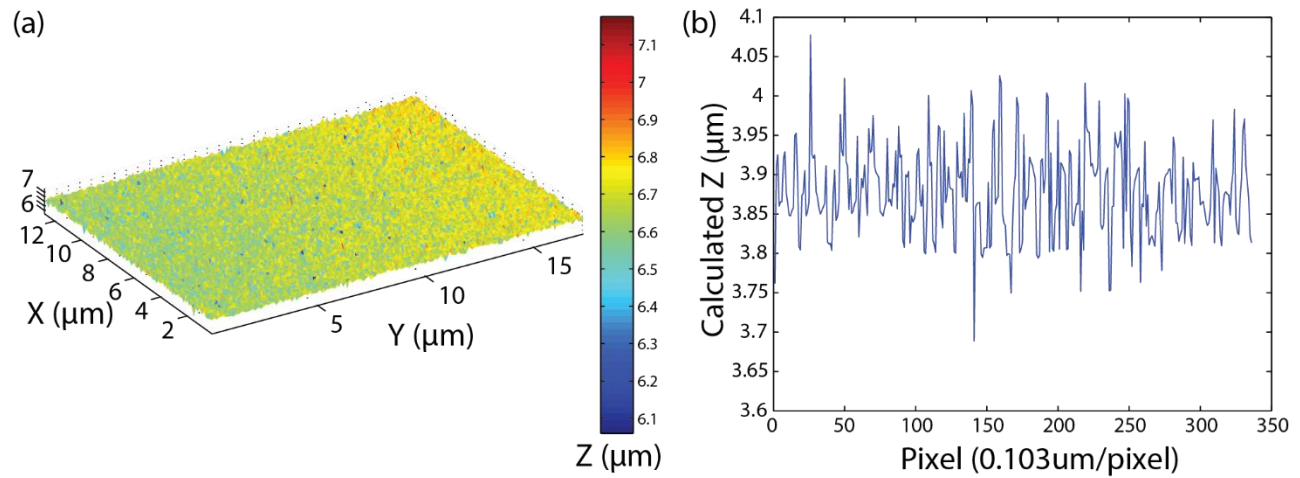
Supplementary Figure S2 Nanopillar-induced nuclear deformation is evident in live NIH3T3 cells transfected with GFP-lamin A. (a) Nuclear deformation is clear on nanopillar array with 75 nm radius, 3 μm pitch, and 1.4 μm height. From left to right: Differential interfering contrast image showing nanopillar locations, Projection of confocal fluorescence from GFP-lamin A, Reconstructed surface of nuclear envelope interacting with nanopillar surface. (b) Nuclear deformation is clear on nanopillar array with 100 nm radius, 3 μm pitch, and 2 μm height. From left to right: Differential interfering contrast image showing nanopillar locations, Projection of confocal fluorescence from GFP-Sun2, Reconstructed surface of nuclear envelope interacting with nanopillar surface.



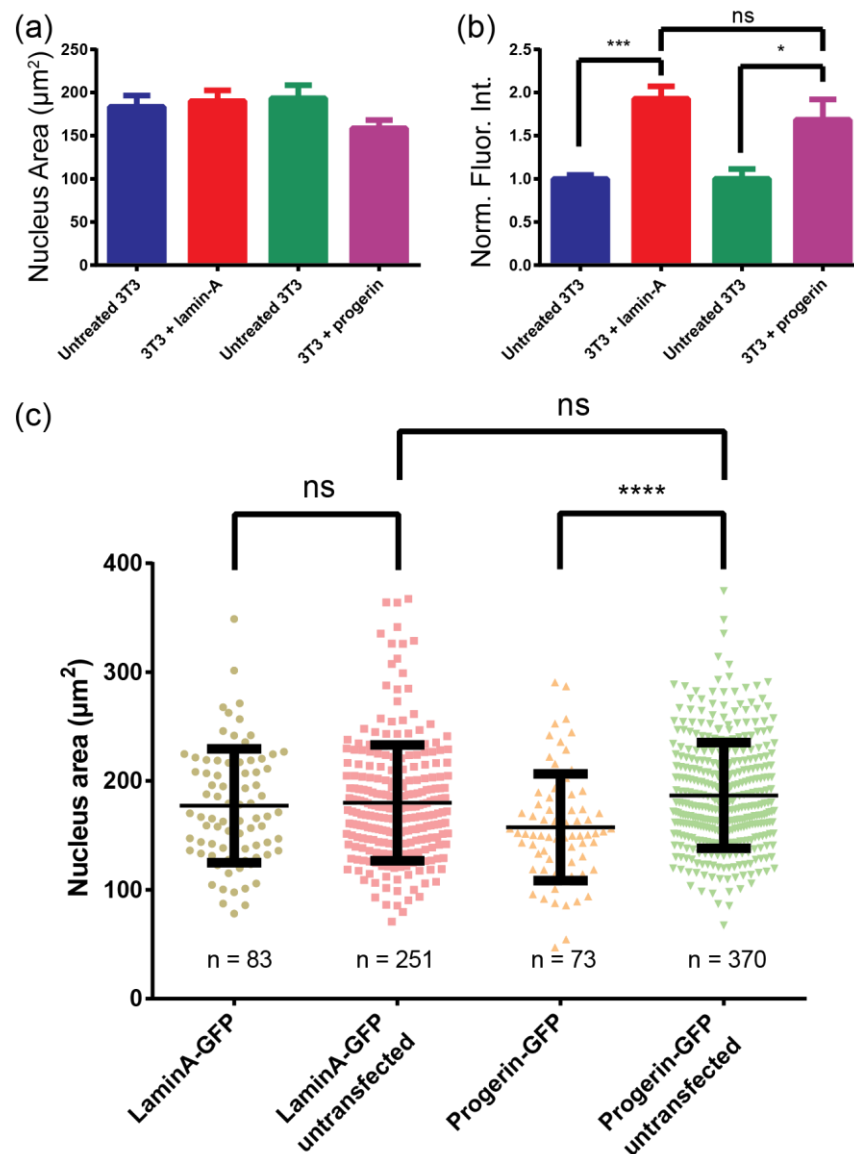
Supplementary Figure S3 Example of occasional trenching behavior of the nuclear envelope on nanopillars. (a) Differential interfering contrast image, showing locations of nanopillars. Dashed green lines indicate the locations of the vertical slices shown in (c). (b) Calculated Z surface reconstruction of nuclear envelope. Trenches are visible between bottom two rows of nanopillars. (c) Confocal fluorescence images of anti-lamin A showing nuclear envelope. Upper left shows horizontal slice, right and bottom show vertical reconstructions. Trenching is evident as the difference in the angle of deformation between the xz and yz vertical reconstructions.



Supplementary Figure S4 Calibration of axial localization accuracy by Gaussian fitting of fluorescent supported lipid bilayer. (a) Calculated surface of lipid bilayer over $200 \mu\text{m}^2$. Colorbar shows vertical range. (b) Line plot through calculated Z of lipid bilayer. Root mean square deviation from the mean is 60 nm.

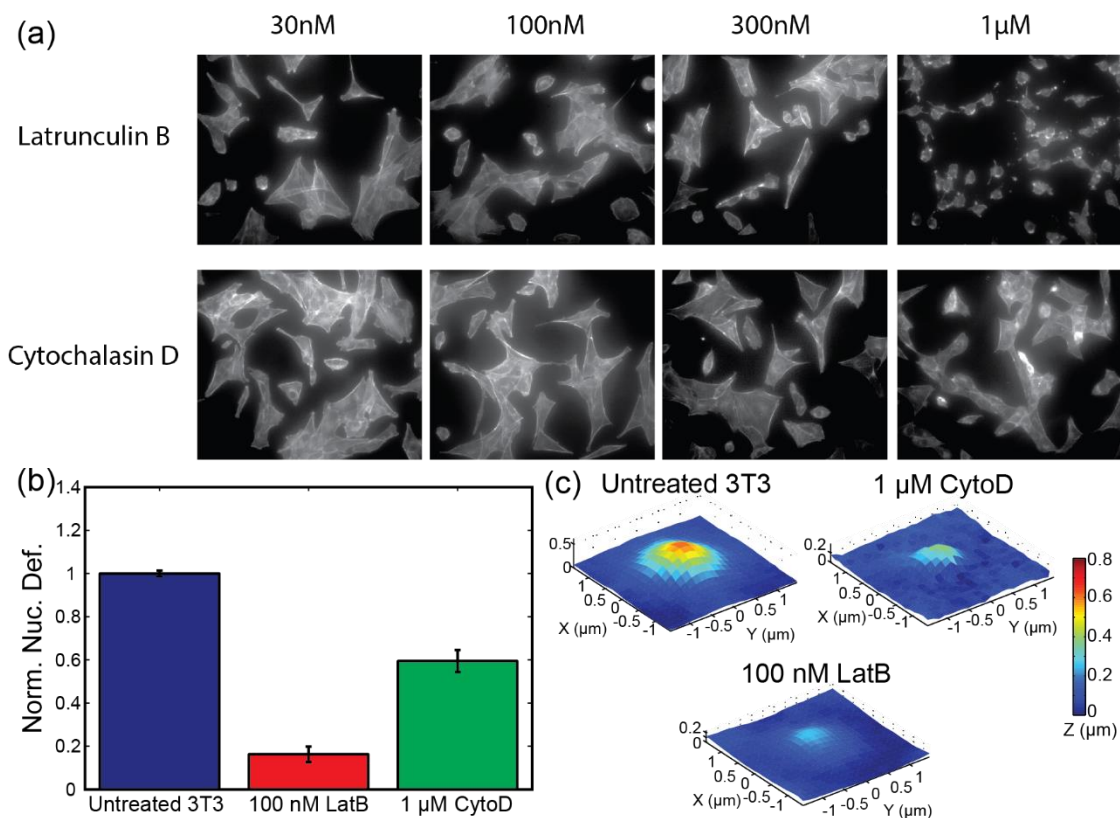


Supplementary Figure S5 GFP-lamin A transfection does not alter nuclear size, but GFP-progerin-transfected nuclei are slightly smaller than untransfected nuclei. (a) Average nucleus area of cells on nanopillars. (b) Fluorescence intensity from anti-lamin A staining is significantly brighter in GFP-lamin A transfected cells and GFP-progerin transfected cells than in untransfected cells. (c) Average nucleus area in large cohort of cells on a flat substrate shows same trend as small sample on nanopillars. There is no significant difference in nuclear size between untransfected cells and GFP-lamin A-transfected cells, but GFP-progerin-transfected nuclei show decreased area. All measurements performed in duplicate and analyzed by one-way ANOVA with Tukey's post test to account for multiple comparisons. ns = no significant difference; * $P < 0.05$; ** $P < 0.01$; *** $P < 10^{-3}$; **** $P < 10^{-4}$.

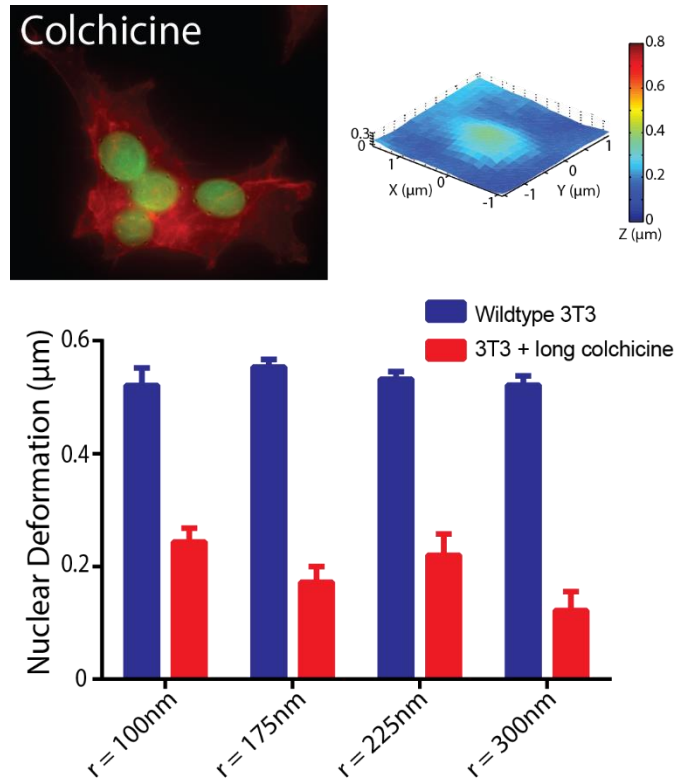


Supplementary Figure S6 Cytochalasin D and Latrunculin B, both inhibitors of actin polymerization, decrease nanopillar-induced nuclear deformation.

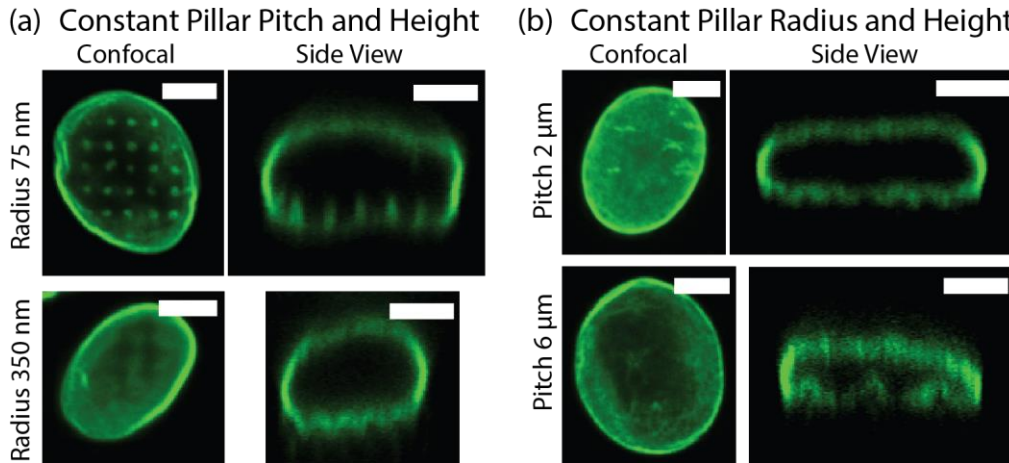
(a) Effect of Latrunculin B and Cytochalasin D on cell and actin morphology. Latrunculin B is effective at lower concentrations. (b) Latrunculin B (100 nM) and Cytochalasin D (1 μ M) decrease depth of nanopillar-induced nuclear deformation. The latrunculin B sample includes the data in Figure 3 as well as two other radii; in all, nanopillars with 100 nm, 180 nm, 220 nm, and 300 nm radius, all 3 μ m pitch and 1.4 μ m height. The Cytochalasin D sample includes nanopillars with 300 nm radius, 3 μ m pitch and 1.4 μ m height, as well as 100 nm radius, 3 μ m pitch and 2 μ m height. Data from each geometry were normalized to the deformation in untreated cells to determine the average effect independent of nanopillar geometry. (c) Average deformed surfaces of nanopillar-induced nuclear deformation in untreated cells and cells treated with 1 μ M Cytochalasin D or 100 nM Latrunculin B for one hour. All three surfaces were averaged from nanopillars with 300 nm radius, 3 μ m pitch and 1.4 μ m height.



Supplementary Figure S7 One hour colchicine treatment disrupts actin and decreases nuclear deformation. (a) Fluorescent image with actin (red) and lamin A (green) staining. Scale bar indicates 10 μm . (b) Average surface of nucleus over nanopillar after 1 hour colchicine treatment. (c) Comparison of average nuclear deformation in untreated 3T3 cells to that after 10 minute colchicine and 1 hour colchicine treatments. Error bars indicate standard error of the mean.

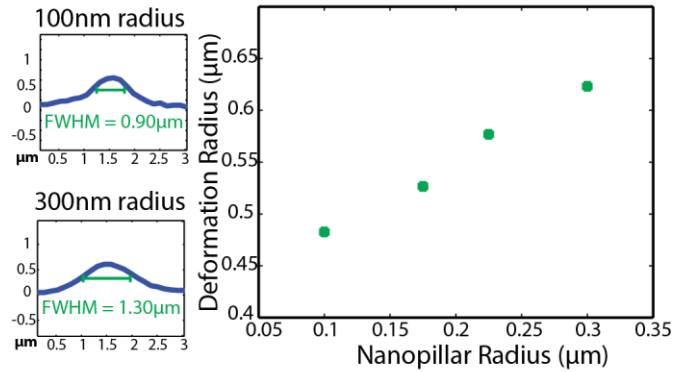


Supplementary Figure S8 Example confocal fluorescence images from nanopillar geometry tests. (a) Nuclear deformation varies with nanopillar radius. Top, radius 75 nm; below, radius 350 nm. On the left are example confocal slices, on the right are side-view reconstructions. (b) Nuclear deformation varies with nanopillar pitch. Top, pitch 2 μm ; below, pitch 6 μm . On the left are example confocal slices, on the right are side-view reconstructions.

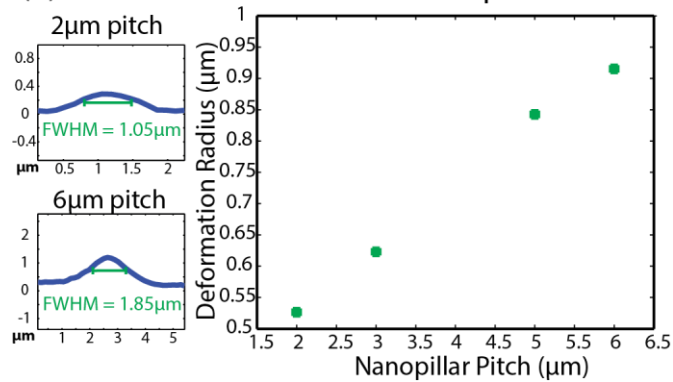


Supplementary Figure S9 Width of nuclear deformation vary with nanopillar radius and pitch. (a) Full width half max (FWHM) of nuclear deformation versus nanopillar radius. Height (1.4 μm) and pitch (3 μm) were held constant for all data points. (b) FWHM of nuclear deformation versus nanopillar pitch. Height (1.4 μm) and radius (300 nm) were held constant for all data points.

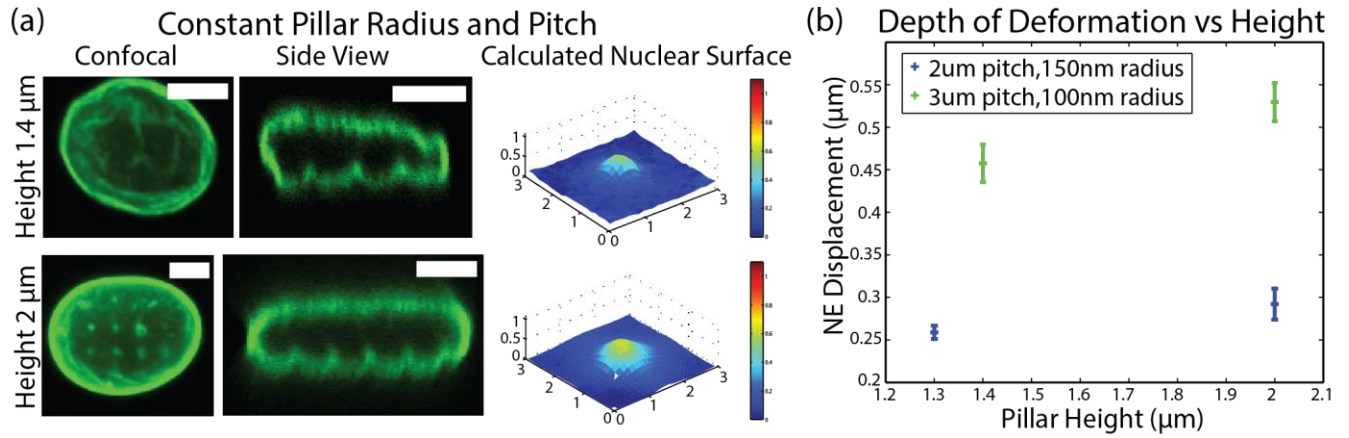
(a) Width of Deformation vs Nanopillar Radius



(b) Width of Deformation vs Nanopillar Pitch



Supplementary Figure S10 Nanopillar height shows a modest effect on nuclear deformation. (a) Example confocal images, side-view reconstructions and calculated nuclear surfaces on nanopillars with the same radius and pitch, at 1.4 μm and 2 μm height. (b) Depth of nuclear deformation versus nanopillar height.



Supplementary Table S2. Material properties for mechanical simulation.

Property	Nucleoplasm	Nuclear Lamina	Nuclear Envelope	Merged Nuclear Envelope
Thickness	4 μm	$t_{\text{NL}} = 25 \text{ nm}$	$t_{\text{b}} = 15 \text{ nm}$	$t_{\text{memb}} = 40 \text{ nm}$
Young's Modulus	25 Pa	$E_{\text{NL}} = 138 \text{ kPa}$	$E_{\text{b}} = 330 \text{ kPa}$	$E_{\text{memb}} = 205 \text{ kPa}$
Poisson Ratio (ν)	0.485	0.485	0.485	0.485

Supplementary Figure S11 Localized pressure from actin around nanopillars. Fluorescence profile of actin staining with nanopillar at center.

